

# Jetting Micron-Scale Droplets onto Chemically Heterogeneous Surfaces

J. Léopoldès<sup>1</sup>, A. Dupuis<sup>2</sup>, D.G. Bucknall<sup>1</sup>, J.M. Yeomans<sup>2</sup>

<sup>1</sup> Department of Materials, Oxford University, Oxford OX1 3PH, UK

<sup>2</sup> Department of Physics, Theoretical Physics, 1 Keble Road, Oxford OX1 3NP, UK

October 29, 2018

## Abstract

We report experiments investigating the behaviour of micron-scale fluid droplets jetted onto surfaces patterned with lyophobic and lyophilic stripes. The final droplet shape is shown to depend on the droplet size relative to that of the stripes. In particular when the droplet radius is of the same order as the stripe width, the final shape is determined by the dynamic evolution of the drop and shows a sensitive dependence on the initial droplet position and velocity. Lattice Boltzmann numerical solutions of the dynamical equations of motion of the drop provide a close quantitative match to the experimental results. This proves helpful in interpreting the data and allows for accurate prediction of fluid droplet behaviour for a wide range of surfaces.

## 1 Introduction

This paper presents a combined experimental and numerical investigation of the behaviour of micron-scale fluid droplets jetted onto chemically patterned surfaces.<sup>1,2</sup> It was motivated by questions of relevance to ink-jet printing where substrates with chemical or physical defects can cause the expected spherical shape of jetted droplets to become distorted, thus affecting the integrity and quality of an image. However, the results have much wider implications in the generic behaviour of fluid droplets on heterogeneous surfaces. This is of particular interest since patterned surfaces are used in wide

diversity of areas such as electronic devices, biologically active substrates or semiconductor nanostructures.

Previous work on the behaviour of fluids on chemically patterned substrates has predominantly concentrated on the equilibrium shape of the drops.<sup>3</sup> In particular there has been extensive theoretical and experimental work on the extent to which the line tension affects droplet shape.<sup>4,5,6,7</sup> Several authors have considered the equilibrium configuration of a fluid on one or two completely wetting stripes in a non-wetting matrix<sup>8,9,10,11,12,13,14,15</sup> and there is recent work describing how such a fluid moves along such a stripe.<sup>16</sup> By contrast, this paper describes the behaviour of fluid droplets on chemically patterned surfaces when the fluid is jetted onto the surface (non-zero impact velocity). This offers new perspectives regarding the achievement of structures impossible to obtain by simple droplet deposition.

The experimental results are compared to numerical simulations achieved by a lattice Boltzmann solution of the equations of motion for a one-component, two-phase fluid. Lattice Boltzmann models are a class of numerical techniques ideally suited to probing the behaviour of fluids on mesoscopic length scales.<sup>17</sup> Several lattice Boltzmann algorithms for a liquid-gas system have been reported in the literature.<sup>18,19,20</sup> They solve the Navier-Stokes equations of fluid flow but also input thermodynamic information, typically either as a free energy or as effective microscopic interactions. They have proved successful in modelling such diverse problems as fluid flows in complex geometries,<sup>21</sup> two-phase models,<sup>18,19</sup> hydrodynamic phase ordering<sup>22</sup> and sediment transport in a fluid.<sup>23</sup>

We consider a one-component, two-phase fluid and use the free energy model originally described by Swift et al.<sup>18</sup> with a correction to ensure Galilean invariance.<sup>24</sup> The advantage of this approach for the wetting problem is that it allows us to tune equilibrium thermodynamic properties such as the surface tension or static contact angle to agree with analytic predictions. Thus it is rather easy to control the wetting properties of the substrate.

Choosing fluid parameters such as viscosity, surface tension and contact angles to match the experimental values we obtain a close quantitative match to the different droplet shapes thus helping to understand the mechanisms for their formation. The results show the importance of dynamic and metastability effects in determining the shapes formed by small droplets on heterogeneous substrates. In particular we demonstrate that the final droplet configuration depends on the droplet size relative to that of the stripes, the initial point of impact and the incident droplet velocity.

## 2 Experimental Section

### 2.1 Fluid

The solventless UV cure black ink-jet ink used (acrylate monomer) has a viscosity of 25.0 mPa.s and a surface tension of 24.4 mN.m<sup>-1</sup>. The droplets were jetted using a 256 nozzle industrial inkjet printhead held 1 mm from the substrate. The print pattern was configured so that the droplets impacted on the surface with an average separation between each drop of 280  $\mu\text{m}$ , at a velocity of 8 m.s<sup>-1</sup>. The ink droplets were cured 1.6 s after ejection from the print head using a standard mercury H UVA lamp system. The radius of the droplets before impact was chosen to be 22  $\mu\text{m}$ , and the typical spreading time of the droplets is of order milliseconds.

### 2.2 Preparation of the substrates

Surfaces are produced with areas of different wettabilities using standard microcontact printing techniques. This is nowadays a well established method, and abundant literature can be found on the subject.<sup>1</sup> The chemical patterns are created on gold coated silicon (001) wafers to make certain that the substrates are molecularly flat, thereby ensuring any effects observed in the droplet behaviour resulted from chemical rather topographic (or a combination of both) effects. Prior to gold evaporation, the wafers are coated with 50 nm chromium to ensure stability of the gold (100 nm). The samples are washed with ethanol and dried with a stream of  $N_2$  before patterning.

The stripes are created using solutions of 4 mmol of either methyl- or carboxyl- terminated octadecyl thiols, which produced lyophobic ( $-\text{CH}_3$ ) and lyophilic ( $-\text{COOH}$ ) monolayer regions on the Au surface. To achieve this, a polydimethylsiloxane stamp is moulded on a master having the desired pattern, and allowed to cure for one week at room temperature. Then a known quantity of hexadecanethiol solution (4 mmol in hexane) is poured onto the elastomeric stamp. After 10 seconds and drying with a stream of  $N_2$ , the stamp is applied onto the surface of the wafer.

This produces a lyophobic self assembled monolayer (SAM) with the desired pattern. The sample is then immersed one hour in a mercapto undecanoic acid / ethanol solution (4mmol) in order to complete the patterning.

The corresponding contact angles for the commercially available black UV cure jet-ink used in these experiments are respectively 64° and 5° on the

Table 1: Widths of the chemically patterned stripes used in this study, as determined by scanning electron microscopy. The sample numbering corresponds to that used in Figure 1.

Sample	lyophilic ( $\mu\text{m}$ )	lyophobic ( $\mu\text{m}$ )
S1	5	56
S2	13	65
S3	19	35
S4	26	47
S5	23	38
S6	50	50
S7	47	31
S8	83	75

lyophobic and lyophilic areas. The contact angles are determined by optical measurement of the equilibrium shape of equivalent sized droplets on surfaces homogeneously produced by solution casting the relevant thiol. The widths of the stripes created by the microcontact printing process, and measured using scanning electron microscopy, are listed in Table 1.

### 3 The lattice Boltzmann model

The lattice Boltzmann approach solves the Navier-Stokes equations by following the evolution of partial distribution functions  $f_i$  on a regular,  $d$ -dimensional lattice formed of sites  $\mathbf{r}$ . The label  $i$  denotes velocity directions and runs between 0 and  $z$ .  $DdQz + 1$  is a standard lattice topology classification. The  $D3Q15$  lattice topology we use here has the following velocity vectors  $\mathbf{v}_i$ :  $(0, 0, 0)$ ,  $(\pm 1, \pm 1, \pm 1)$ ,  $(\pm 1, 0, 0)$ ,  $(0, \pm 1, 0)$ ,  $(0, 0, \pm 1)$  in lattice units.

The lattice Boltzmann dynamics are given by

$$f_i(\mathbf{r} + \Delta t \mathbf{v}_i, t + \Delta t) = f_i(\mathbf{r}, t) + \frac{1}{\tau} (f_i^{eq}(\mathbf{r}, t) - f_i(\mathbf{r}, t)) \quad (1)$$

where  $\Delta t$  is the time step of the simulation,  $\tau$  the relaxation time and  $f_i^{eq}$  the equilibrium distribution function which is a function of the density  $n = \sum_{i=0}^z f_i$  and the fluid velocity  $\mathbf{u}$  defined through the relation  $n\mathbf{u} = \sum_{i=0}^z f_i \mathbf{v}_i$ .

The relaxation time tunes the kinematic viscosity as<sup>17</sup>

$$\nu = \frac{\Delta \mathbf{r}^2 C_4}{\Delta t C_2} \left( \tau - \frac{1}{2} \right) \quad (2)$$

where  $\Delta \mathbf{r}$  is the lattice spacing and  $C_2$  and  $C_4$  are coefficients related to the topology of the lattice. These are equal to 3 and 1 respectively when one considers a  $D3Q15$  lattice (see<sup>25</sup> for more details).

It can be shown<sup>18</sup> that equation (1) reproduces the Navier-Stokes equations of a non-ideal gas if the local equilibrium functions are chosen as

$$\begin{aligned} f_i^{eq} &= A_\sigma + B_\sigma u_\alpha v_{i\alpha} + C_\sigma \mathbf{u}^2 + D_\sigma u_\alpha u_\beta v_{i\alpha} v_{i\beta} + G_{\sigma\alpha\beta} v_{i\alpha} v_{i\beta}, \quad i > 0, \\ f_0^{eq} &= n - \sum_{i=1}^z f_i^{eq} \end{aligned} \quad (3)$$

where Einstein notation is understood for the Cartesian labels  $\alpha$  and  $\beta$  (i.e.  $v_{i\alpha} u_\alpha = \sum_\alpha v_{i\alpha} u_\alpha$ ) and where  $\sigma$  labels velocities of different magnitude. A possible choice of the coefficients is<sup>26</sup>

$$\begin{aligned} A_\sigma &= \frac{w_\sigma}{c^2} \left( p_b - \frac{\kappa}{2} (\partial_\alpha n)^2 - \kappa n \partial_{\alpha\alpha} n + \nu u_\alpha \partial_\alpha n \right), \\ B_\sigma &= \frac{w_\sigma n}{c^2}, \quad C_\sigma = -\frac{w_\sigma n}{2c^2}, \quad D_\sigma = \frac{3w_\sigma n}{2c^4}, \\ G_{1\gamma\gamma} &= \frac{1}{2c^4} \left( \kappa (\partial_\gamma n)^2 + 2\nu u_\gamma \partial_\gamma n \right), \quad G_{2\gamma\gamma} = 0, \\ G_{2\gamma\delta} &= \frac{1}{16c^4} \left( \kappa (\partial_\gamma n) (\partial_\delta n) + \nu (u_\gamma \partial_\delta n + u_\delta \partial_\gamma n) \right) \end{aligned} \quad (4)$$

where  $w_1 = 1/3$ ,  $w_2 = 1/24$ ,  $c = \Delta \mathbf{r} / \Delta t$ ,  $\kappa$  is a parameter related to the surface tension and  $p_b = p_c (\nu_p + 1)^2 (3\nu_p^2 - 2\nu_p + 1 - 2\beta\tau_p)$  is the pressure in the bulk where  $\nu_p = (n - n_c) / n_c$ ,  $\tau_p = (T_c - T) / T_c$  and  $p_c = 1/8$ ,  $n_c = 3.5$  and  $T_c = 4/7$  are the critical pressure, density and temperature respectively and  $\beta$  is a constant typically equal to 0.1.

The derivatives in the direction normal to the substrate are handled in such a way that the wetting properties of the substrate can be controlled. A boundary condition can be established using the Cahn model.<sup>27</sup> He proposed adding an additional surface free energy  $\Psi_c(n_s) = \phi_0 - \phi_1 n_s + \dots$  at the solid surface where  $n_s$  is the density at the surface. Neglecting the second order terms in  $\Psi_c(n)$  and minimizing  $\Psi_b + \Psi_c$  (where  $\Psi_b$  is the free energy in the bulk), a boundary condition valid at  $z = 0$  emerges

$$\partial_z n = -\frac{\phi_1}{\kappa}. \quad (5)$$

Equation (5) is imposed on the substrate sites to implement the Cahn model in the lattice Boltzmann approach. Details are given in.<sup>28</sup>

The Cahn model can be used to relate  $\phi_1$  to  $\theta$  the contact angle defined as the angle between the tangent plane to the droplet and the substrate<sup>26</sup>

$$\phi_1 = 2\beta\tau_p\sqrt{2p_c\kappa} \operatorname{sign}\left(\theta - \frac{\pi}{2}\right)\sqrt{\cos\frac{\alpha}{3}\left(1 - \cos\frac{\alpha}{3}\right)} \quad (6)$$

where  $\alpha = \cos^{-1}(\sin^2\theta)$  and the function sign returns the sign of its argument.

We impose a no-slip boundary condition on the velocity. Because the full dynamics takes place on the boundary the usual bounce-back condition must be extended to ensure mass conservation (see<sup>25</sup> for a wider discussion). This is done by a suitable choice of the rest field,  $f_0$ , to correctly balance the mass of the system.

This model reproduces Young's law and the expected dependence of the droplet behaviour on viscosity and surface tension.<sup>26</sup>

The following lattice Boltzmann parameters are set. The initial droplet radius  $R_0 = 30$  lattice sites. The droplet is initialised with a vertical velocity equal to  $U_0 = 0.02$ . The lattice geometry is  $L_x \times L_y \times L_z$  where  $L_x$  and  $L_y$  are chosen large enough to not affect the behaviour of the droplet and  $L_z = 40$ . The relaxation time  $\tau = 0.63$ . The surface tension related parameter  $\kappa = 0.0012$ . The temperature  $T = 0.4$  which leads to two phases of density  $n_l = 4.128$  and  $n_g = 2.913$ . The simulations are run for 400 000 iterations.

Simulation and physical parameters are related as usual by choosing a length scale  $L_0$ , a time scale  $T_0$  and a mass scale  $M_0$ . A simulation parameter with dimensions  $[L]^{n_1}[T]^{n_2}[M]^{n_3}$  is multiplied by  $L_0^{n_1}T_0^{n_2}M_0^{n_3}$  to give the physical value.  $L_0 = 1.5 \cdot 10^{-6}m$ ,  $T_0 = 3.7 \cdot 10^{-9}s$  and  $M_0 = 7.9 \cdot 10^{-16}kg$  were chosen to give physically realistic droplet diameter, viscosity and surface tension.

## 4 Results and discussion

A top view of the final droplet shapes on the different patterned surfaces is shown in Figure 1. To our knowledge, it is the first time that the evolution of droplet shape has been studied over such a large range of heterogeneities.

When the width of the stripes is much smaller than the droplet radius ( $S1$ ) the contact line is almost circular with only small deviations near the

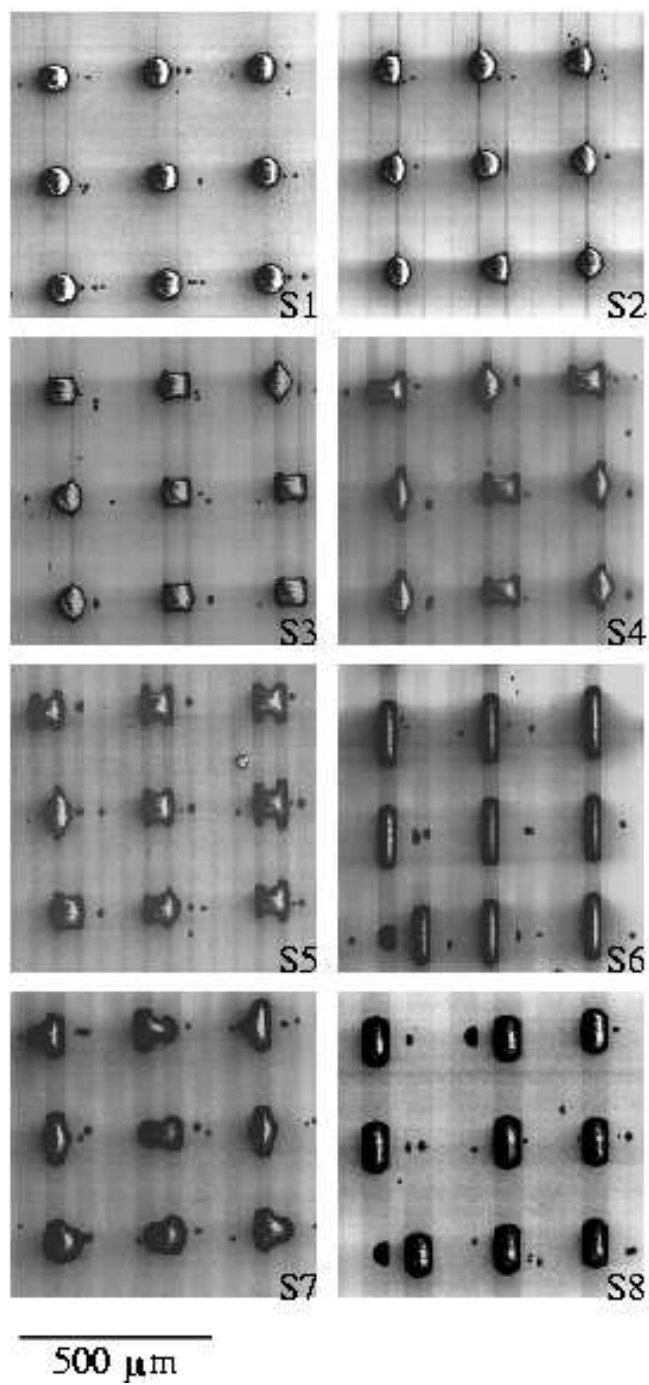


Figure 1: Scanning electron micrographs of inkjet droplets on patterned surfaces. Lyophilic and lyophobic stripes appear dark and pale respectively.<sup>29</sup> The stripe widths for the different samples are listed in Table 1.

stripe boundaries as previously reported in the literature.<sup>4,5</sup>

For wider stripes, where the dimensions are now approaching the droplet diameter, the fluid remains confined to a lyophilic region (*S6*, *S8*) and the final shape is therefore highly elongated.

It should also be noted that in samples *S6* and *S8*, the regular droplet pattern array is disrupted as droplets can be displaced to the neighbouring lyophilic region. When this occurs, a small portion of the initial droplet volume can remain on a neighbouring lyophilic stripe.

In the intermediate cases, for droplets impinging on the stripes *S3*, *S4*, *S5* and *S7*, two different characteristic droplet shapes are observed: "lozenge" or "butterfly".

The reason for the formation of these shapes can be understood by considering a lattice Boltzmann modelling of the droplet dynamics.

Figure 2(a) shows the droplet contact lines for intermediate and equilibrium stages of the droplet wetting as a function of the initial impact position of the jetted fluid. The modelled substrate is defined so that the surface heterogeneities are equivalent with the sample *S4*. The droplet at the point of impact is assumed to be spherical with an imposed velocity equal to that used experimentally ( $8 \text{ m}\cdot\text{s}^{-1}$ ). It is quite clear that the shapes obtained by such calculations are entirely consistent with those obtained experimentally. The very strong similarities are more clearly demonstrated in Figure 2(b) where the experimental and numerical simulations are overlaid for the two equilibrium droplet shapes. The good quantitative agreement between the simulations and the experimental results is extremely pleasing given that all the parameters in the simulation are fixed by the physical conditions dictated by the experiments. Small differences are not surprising because of the uncertainty in the experimental values of the transport coefficients and surface energies, and the possibility of contact line pinning on real substrates.

Note in particular that, just as in the experiments, two different final droplet shapes are obtained in the numerical modelling for the substrate geometry *S4*.

The simulations allow us to follow the dynamical pathway by which the final equilibrium states are reached. Consider case 1 (see Figure 2(a)) where the initial contact point of the droplet is in the centre of a lyophilic stripe. The drop initially evolves symmetrically parallel and normal to the stripe. Once the boundary of the lyophobic stripe is reached horizontally, the fluid moves more quickly along the lyophilic than along the lyophobic part of the substrate. Note that there is an overshoot of the fluid in the direction



perpendicular to the stripes (the maximum extent of the contact line exceeds that of the equilibrium droplet). This occurs as the droplet initially spreads due to its impact velocity, and relaxes to its equilibrium shape determined by the wetting behaviour. The net effect is an equilibrium shape which has a distinctive lozenge shape centred over a lyophilic stripe.

Now consider case 2 where the droplet strikes the substrate in the middle of a lyophobic stripe. Because the initial diameter is approximately the same as that of the lyophobic stripes, the droplet spreads directly onto adjacent lyophilic parts of the substrate giving the characteristic butterfly shape which is symmetrically located over two lyophilic and one lyophobic stripes.

When the droplet impacts on a location other than the middle of a stripe, the symmetry of the evolution parallel to the stripes is lost. Despite this initial asymmetry the final state is always symmetric and produces either the characteristic lozenge (for the initial positions 3, 5 and 6) or butterfly (for the initial position 4) patterns. These states correspond to long lived metastable or stable equilibria.<sup>14</sup> The numerical results give a free energy for the butterfly-shaped droplets which is  $\sim 1\%$  of the lozenge free energy.

Figure 2(a) also allows us to predict that jetting droplets onto substrate *S4* should lead to approximately equal numbers of lozenge and butterfly shapes. Numerical results show that a droplet spreads into a lozenge if it hits the surface on a lyophilic stripe or its close surroundings (up to about one eighth of the width of the neighbouring lyophobic stripes). This corresponds to about half the substrate area and therefore one expects about one half of the droplets to take each of the final shapes consistent with the experimental results for *S4*, as shown in

Figure 1. Thus far we have shown that the parameters affecting the final shape of a drop impacting on a striped substrate are the relative sizes of the drop and the stripes and the initial point of impact.

Clearly, the surface energies of the different stripes will have an important effect on the droplet spreading behaviour,<sup>14</sup> and given the results described above the initial drop velocity may also be important.

To test the latter, numerical simulations comparing the time evolution of a drop with and without impact velocity have been undertaken (see Figure 3). The final state is indeed different, as the drop with no impact velocity is unable to reach, and hence take advantage of the wetting possibilities of the neighbouring lyophilic regions of the substrate. For a given average distance between heterogeneities, the droplet velocity appears to be an important parameter regarding to the number of surface heterogeneities encountered

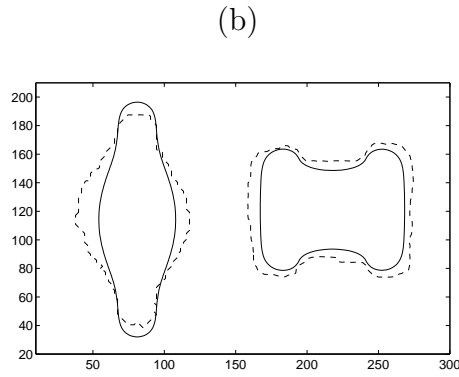
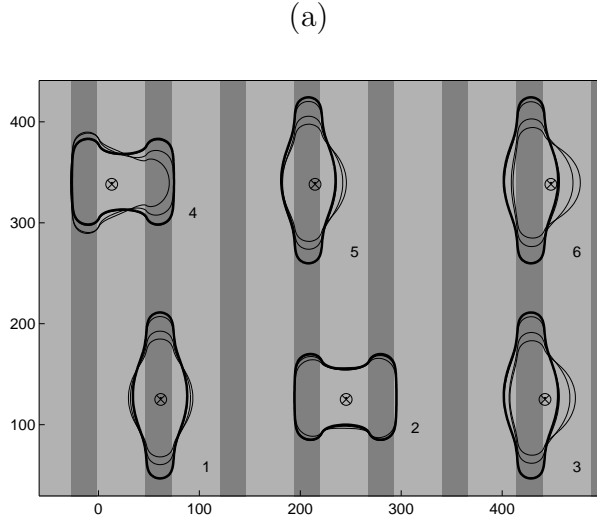


Figure 2: The modelled substrate is defined so that the surface heterogeneities are equivalent with the sample  $S4$ . (a) Numerical simulation of droplets hitting the surface at various impact points indicated by encircled crosses. For each droplet the bold and faint lines represent the extent of the droplet at equilibrium and at intermediate times, respectively. The lyophobic and lyophilic regions are shaded to be consistent with Figure 1. (b) Direct comparison between experimental ( $S4$ , dashed lines) and numerical (solid lines) equilibrium contact lines. The length scales in both plots are reported in micrometers.

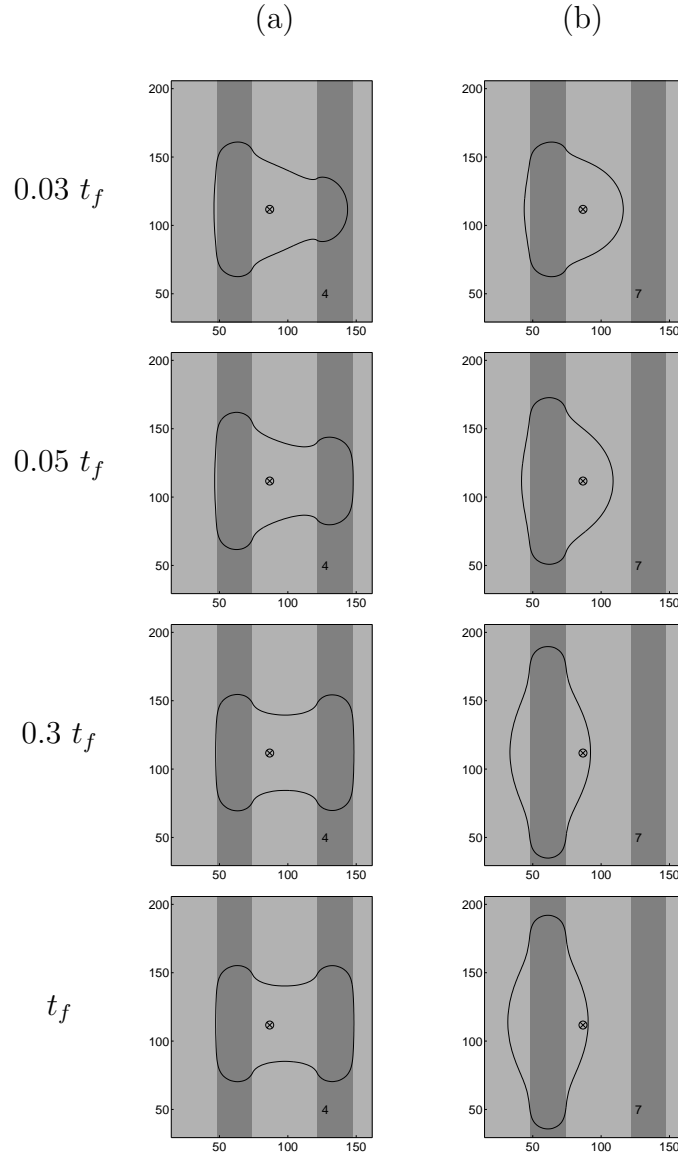


Figure 3: Time evolution (top to bottom) of the droplet shape from numerical simulations of the equations of motion. (a) Droplet spreading with impact velocity  $8 \text{ ms}^{-1}$ . (b) No impact velocity. The initial point of impact is the same for both simulations.  $t_f$  is the final simulation time.

during spreading.

## 5 Conclusion

We have presented experimental and numerical results investigating the behaviour of micron-scale droplets on chemically patterned substrates. When the drop radius is of the same order as the stripe width the final droplet shape is determined by the dynamic evolution of the drop and is very sensitive to the initial droplet position and velocity. The final state may be metastable and is not determined just by a minimisation of the free energy.

We have shown that it is possible to provide a close quantitative correspondence between numerical solutions of the hydrodynamic equations of motion describing the spreading and the experimental results. This has proved invaluable in fully understanding the data and in predicting droplet behaviour for parameter values not available experimentally.

These results underline the difficulties inherent in controlling the details of patterns formed using ink-jet printing (where the underlying substrate is likely to have both chemical and topological heterogeneities) and the subtle effects of the surface wetting properties on the behaviour of liquids on patterned substrates. The present work will therefore be extended to topological surface features and complex fluids.

## Acknowledgments

We gratefully thank Dr. G. Desie and S. Allaman (Agfa Research Center, Belgium) for their collaboration. Dr. H. Zhang is acknowledged for allowing us to use the PDMS stamp. This work forms part of the IMAGE-IN project which is funded by the European Community through a Framework 5 grant GRD1-CT-2002-00663.

## References

- [1] Y. Xia and G. M. Whitesides. *Angew. Chem. Int.*, 37:550–575, 1998.
- [2] H. Sirringhaus, T. Kawase, R.H. Friend, T. Shimoda, and M. Inbasekaran. *Science*, 290:2123–2126, 2000.

- [3] A. B. D. Cassie. *Discuss. Faraday Soc.*, 3:11, 1948.
- [4] J. Drelich, J. L. Wilbur, J. D. Miller, and G. M. Whitesides. *Langmuir*, 12(7):1913–1922, 1996.
- [5] J. Drelich, J. D. Miller, A. Kumar, and G. M. Whitesides. *Coll. Surf., A: Physicochem. Eng. Aspects*, 93:1, 1994.
- [6] T. Pompe, A. Fery, and S. Herminghaus. *Langmuir*, 14(10):2585–2588, 1998.
- [7] J. Buerhle, S. Herminghaus, and F. Mugele. *Langmuir*, 18:9771–9777, 2002.
- [8] P. G. de Gennes and J. F. Joanny. *J. Chem. Phys.*, 81(1):552–562, July 1984.
- [9] M. E. R. Shanahan. *Coll. and Surf. A: Physicochem. Eng. Aspects.*, 156:71–77, 1999.
- [10] D. Li. *Coll. and Surf. A: Physicochem. Eng. Aspects*, 116:1–23, 1996.
- [11] A. A. Darhuber, S. M. Troian, and S. M. Miller. *J. Appl. Phys.*, 87(11):7768–7775, 2000.
- [12] P. Lenz. *Adv. Mater.*, 11(18):1531–1534, 1998.
- [13] R. Lipowsky. *Curr. Opin. Colloid Interface Sci.*, 6:40–48, 2001.
- [14] M. Brinkmann and R. Lipowsky. *J. Appl. Phys.*, 92(8):4296–4306, 2002.
- [15] C. Bauer and S. Dietrich. *Phys. Rev. E*, 60(6):6919–6941, 1999.
- [16] A. A. Darhuber, S. M. Troian, and W. W. Reisner. *Phys. Rev. E*, 64:031603, 2001.
- [17] S. Succi. *The Lattice Boltzmann Equation, For Fluid Dynamics and Beyond*. Oxford University Press, 2001.
- [18] M.R. Swift, E. Orlandini, W.R. Osborn, and J.M. Yeomans. Lattice Boltzmann simulations of liquid-gas and binary fluid systems. *Phys. Rev. E*, 54:5051–5052, 1996.

- [19] X. Shan and H. Chen. *Phys. Rev. E*, 47:1815–1819, 1993.
- [20] X. He, S. Chen, and G.D. Doolen. *J. Comput. Phys.*, 146:282–300, 1998.
- [21] F. Higuera, S. Succi, and E. Foti. *EuroPhysics Letters*, 10(5):433–438, 1989.
- [22] V.M. Kendon, J.C. Desplat, P. Bladon, and M.E. Cates. *Phys. Rev. Lett.*, 83(3):576–579, 1999.
- [23] A. Dupuis and B. Chopard. *J. Comput. Phys.*, 178(1):161–174, 2002.
- [24] D. Holdych, D. Rovas, J. Georgiadis, and R. Buckius. *Int. J. Mod. Phys. C*, 9:1393–1404, 1998.
- [25] A. Dupuis. *From a lattice Boltzmann model to a parallel and reusable.* PhD thesis, University of Geneva, <http://cui.unige.ch/spc/PhDs/aDupuisPhD/phd.html>, June 2002.
- [26] A. Dupuis, A. J. Briant, C. M. Pooley, and J. M. Yeomans. In P.M.A Sloot et al., editor, *Proceedings of the ICCS 2003 conference*, pages 1024–1033, St.Petersburg, Russia, 2003. Springer.
- [27] J. W. Cahn. Critical point wetting. *J. Chem. Phys.*, 66:3667–3672, 1977.
- [28] A. J. Briant, P. Papatzacos, and J. M. Yeomans. *Philos. T. Roy. Soc. A 360*, 1792:485–495, Mar 2002.
- [29] N. Saito, Y. Wu, K. Hayashi, H. Sugimura, and O. Takai. *J. Phys. Chem. B*, 107:664–667, 2003.

